ISSN: 0974-5823 Vol. 7 No. 1 January, 2022

International Journal of Mechanical Engineering

Assessment of a parabolic trough collector's thermophysical performance

Mazin Y. Abdul-kareem [1], Suha K. Jebir [2], Ahmed F. Khudheyer [3]

[1,2,3] Al-Nahrain University, Baghdad, Iraq.

Abstract

Using the sun's radiation seems to be a potential way to meet a range of modern current societal energy demands inside the future. The concentrator collectors, the most well-known sunlight focusing device, are presented in this analysis, and it's been shown that work effectively in extreme temps. ANSYS CFX is indeed a commercially available simulation tool that streamlines the process for simulating complicated problems to use the finite volume investigation. Using a parabolic trough collector model, varying operating circumstances may be modeled. Predicting the efficiency of the model and analyzing heat transport processes are also objectives of such a work. One-dimensional prediction simulations are being used to validate the performance gradient. Aside from that, the thermal fluxes concentration on the outer face of the absorbers is being shown, so too is the temperature profile inside the absorbing within the tubes. As a result, the tube's overall heat transfer factor was computed, as well as the comparison is made to simulation values. Angle effectiveness modifiers are used to forecast the improvement the thermal performance under different operational circumstances. These concluding results demonstrated that the PTC model operates well and all predictions have been confirmed by the PTC system.

Keywords: PTC, parabolic, solar energy, trough, concenterator.

Introduction

As a renewable energy source, energy from the sun comprises heated water preparations, conditioning, chemical products as well as heating systems. Mostly on market, there is a lot of use of concentrator catchers (PTC). It's true that there are various alternative models, such as Generators for parabolic solar concentrator's expense and partially capture solar radiations, also were addressed. As the earliest source of energy known to man, the solar system is primarily applied for a wide range of purposes, especially commercial heating water for power generation [1–4], particularly in areas with high solar irradiance levels, such as Italy. As a result of their ability to generate hot temperatures (above 400 °C) and excellent thermal efficiency. Achieving this is just what made these viable and attractive technologies within areas such as Water desalination; Sunlight chemistry; Solar cooling; solar hydrogen generation; and Concentrating Solar Power (CSP) [5-7]. Hyperbolic dishes paired with such a Combustion engine is the most typical solar technology for power generation [8-9], followed by linear Fresnel collector, parabola dishes, and sunny towers (central receivers systems). 90 percent of the overall CSP systems employ Parabolic Dish Collectors (PTC) since this innovation is perhaps the most developed across concentrated collectors; that results in light improving the strength and has been used for periods [11]. These technologies are currently functioning in several positions of great renewable energy possible, such in the United States [12], Algeria [13, 14], and Spain [15]. Evacuated tubes and straight parabolic reflectors are the essential components of a PTC. An evacuated pipe be situated in the line of focus for mirror, which is created by curving reflective strips into a paraboloid. To heat the heated water, a parabolic reflector reflects sun energy onto an outer tube. To continue the growth of CSP systems across the world, generally increased efficiency, as well as efficiency improvements, are required [9,16]. To this end, several types of research have been conducted in this sector, experimenting with new concepts and enhancing the current collector. According to the publications, mathematical simulations, as well as modeling techniques, were also used to study a large number of aspects that impact the PTC's effectiveness. Several studies are studying the enhanced optically assessment of focusing collectors, while Cheng et al. using the Monte Carlo of tracing for ray simulate optically a PTC [20] and Binotti and colleagues [10] using the First optical technique for the visual examination of an investigated model. It was completed by Ouagued et al. [16] by using the Euler technique to solve a set of energy and exergy partial differential equations. Refs. [18-21] used conventional oil nanofluids as the fluid results in greater thermal efficiency between both the absorption and mass flow rate due to the usage of nanoparticles. Number crunching is commonly used in thermal efficiency analyses since it is the easiest numerical approach [22–25]. Liquid water outperforms synthetic oil (TherminolVP-1TM) according to Marie et al. [26]. One-dimensional and three-dimensional heat transport analyses were performed by Gong et al. Three-dimensional investigations have also been published [27, 28]. They constructed a dynamical model to assess the effectiveness of a PTC trendy temporary processes and validated by using results from experiments indicated in literature [31]. With the use of Engineering Equations Solver (EES), several more models were successfully developed against previous data. As an alternative, models utilizing programs abound within literary canon too. A PTC collector's thermal performance was maximized by Tsai and Lin [35] by simulating several types of mirrors in Autodesk [36]. It was concluded that greater thermal conductivity absorbing substances reduce the greatest circumferential temperature gradient and hence enhance thermal performance by Akbarimoosavi and Yaghoubi [36]. On top of all that, FLUENT is a very powerful simulation software that has spawned several publications [37–39]. They are interested in a recent model by Mwesigye et al., [40], which shows that such insertion of valve plate plugs within tubes enhances thermal performance by 1.2 percent while decreasing the absorbing temperature by a substantial amount. Numerous experiments with mathematical verification may be reported in earliest researchs [41–46].

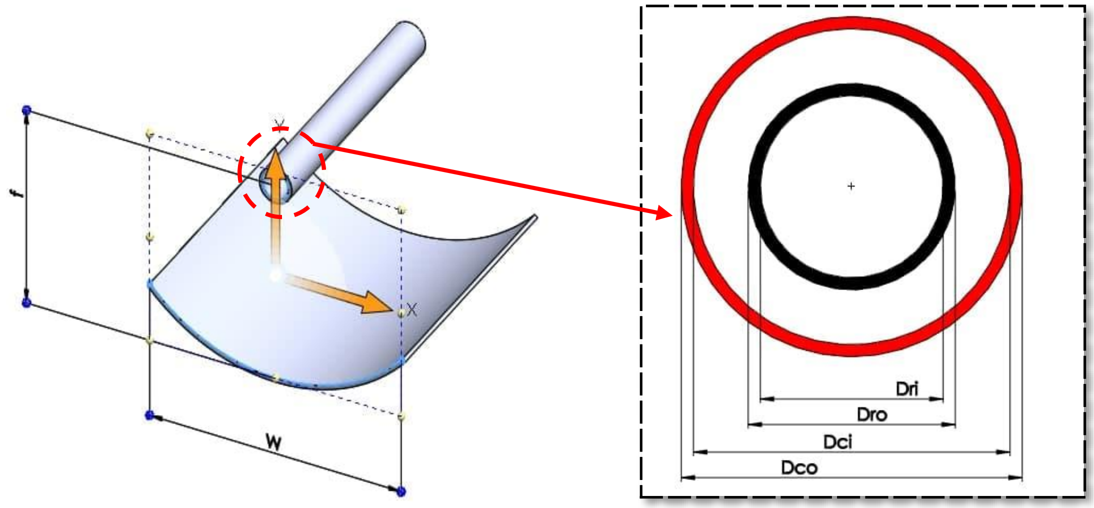

a b

Fig.1 schematic diagram for PTC and absorber tube

When Autodesk had been used to visualize collector of parabolic trough is studied using, in the present research, its utilization effectiveness in various operational circumstances as compared to that of conventional collectors. Many factors go into simulating the functioning of a solar collector. The method takes into consideration all of the observable phenomena such as solar beam reflection and sunny thermal radiation transfer. In addition, a basic 1-D thermal model was built to verify their modeling findings using Autodesk.

Analyses and models of simulation

That research aims to simulate a parabolic trough collector. A tiny methodology was built and evaluated in the Ansys workbench to decrease the calculation time in reducing the computational costs. These results can be extrapolated to a larger model with a comparable concentration ratio, if necessary.

problem description

The parabolic trough collector was developed in Ansys workbench but then just evaluated in Simulation Model Software before it was built and installed. This is shown in Fig. 1a and Fig. 1b. Table 1 lists the major characteristics of this model, as well as the most essential modeling variables, in order of importance. For such heat transfer characteristics, standard values were taken into account to mimic aspects of reality. The simulated requirements are given inside the left column of Table 1, while the fundamental features of the design are listed in the right column. All of these variables have the same levels in all the examples that were studied. Two important parameters must be changed to mimic different working situations: inflow temperature and sun inclination angle in latitude orientation. Throughout this study, the working fluid is pressured water, which is always in a liquid state. Maintaining the liquid phase requires pressure greater than 20 bar and saturation temperatures near 200 °C. Since there are so many instances to investigate, the temperature of the water is varied from 10°C up to 180°C.

Mathematical model

It will find in this section the mathematical concepts formulae of this study. Eq. 1 and solar irradiance in the troughs apertures may be estimated using Eq 2. Note that a PTC relies just on the sunrays to operate.

Table 1
Model dimensions and simulation parameters.

Simulation parameters	**Value**	**Model dimensions**	**Value** (m)
ε_p	0.1	W	0.840
ε_c	0.88	L	1.000
$\rho(\tau\alpha)$	0.8015	f	0.300
G_b	500 W/m^2	D_{ri}	0.020
m	0.02 kg/s	D_{ro}	0.022
T_{am}	10 °C	D_{ci}	0.032
h_{ca}	10 W/m^{2}K	D_{co}	0.034

$$Q_u = \dot{m} \cdot c_p \cdot (T_{out} - T_{in}) \quad (1)$$

$$Q_s = A_a \cdot G_b \quad (2)$$

$$\eta = \frac{Q_u}{Q_s} \quad (3)$$

$$Q_{\text{loss}} = U_L \cdot A_{ro} \cdot (T_r - T_{am}), \quad (4)$$

$$Q_{\text{loss}} = \frac{\sigma \cdot A_{ro} \cdot (T_r^4 - T_c^4)}{\frac{1}{\varepsilon_r} + \frac{1-\varepsilon_c}{\varepsilon_c} \cdot \frac{A_{ro}}{A_{ci}}} \quad (5)$$

$$Q_{\text{loss}} = A_{co} \cdot h_{ca} \cdot (T_c - T_{am}) + \varepsilon_c \cdot A_{co} \cdot \sigma \cdot (T_c^4 - T_{am}^4) \quad (6)$$

the tube surface, or the surface of the cover tube,

$$A_i = \pi \cdot D_i \cdot L \quad (7)$$

Where $i = D_{co}, D_{ci}, D_{ro}, D_{ri}$

Nusselt number for laminar flow can be calculated by using [47],

$$Nu_m = 3.66 + \frac{0.0668 \cdot \text{Re} \cdot \text{Pr} \cdot D_{ri}/L}{1 + 0.04 \cdot (Re \cdot \text{Pr} \cdot D_{ri}/L)^{2/3}} \quad (8)$$

and for turbulent flow,

$$Nu_m = 0.023 \cdot Re^{0.8} \cdot \text{Pr}^{1/3} \quad (9)$$

Convection heat transfer coefficient can be calculated from simulation by,

$$h_w = \frac{Q_u}{(\pi \cdot D_{ri} \cdot L) \cdot (T_r - T_{fm})} \quad (10)$$

The localized concentration ratio is also another expression that is quite important in computations. As a more precise measure, this is the ratio of the theoretically received irradiance for uniformly distributed in every section of the absorbers. According to,

$$C_L = \frac{dQ_{abs}}{\rho \cdot (\tau\alpha) \cdot G \cdot dA} \quad (11)$$

Therefore, the optical effectiveness modification was calculated as follows:

$$K(\theta) = \frac{\eta_{opt}(\theta)}{\eta_{opt}(\theta = 0°)} \quad (12)$$

θ was any transverse angular deviation.

Numerical analysis

Validation of the simulation findings had been done using optimizing compilers 1-D analytical simulations. This system depends just on human metabolism in the absorbers to identify overall usable energy as well as the energy loss to determine the valuable energy and heat losses. This is a reasonable approximation since the tubes are not long and the temperature profile is near the average value. Due to a lack of actual heat transmission mechanisms, it's recommended that covering temperature be adjusted higher than ambient. To calculate water temperature at output section, the energy losses and usable energy are computed and compared to one another. The temperature of the receiver may be measured by manipulative heat transfer features between tube and water. may be used temperature for calculating the cover temperature. A large relaxation factor was required for this technique to be convergent. As a rule of thumb, 20000 iterations were required to accurately estimate the ideal cover temperature.

Grid generation and mesh independent

For the current CFD analysis, Fig. 3(a) depicts the model structure of a standard absorbers. Through establishing a divide on the lower surface of a pipe outer layer, a concentrated heat flux zone is created on the pipe outer surface of the single tube absorber. For the current investigation, the heat flow encroaches on a 5 mm-wide concentrated area. Since accessibility to the lower halfway pipe was restricted, the exact width of the beam that impinges on the bottom mid tube in the tests cannot be measured. ANSYS fluent 2021 preprocessing is used to create hexahedral components over the whole flow domain as shown in Fig.3b. The near wall grid function of a preprocessing is being used to build thinner enhanced wall mesh generation, with the first node at 0.05mm and a preset growth factor of 1.02 for 30 layers. This one is made in order to better reflect the flow behavior near to the walls. Using the surfaces mean water outlet temperature as a grading criterion, array total independence analyses are carried on single tube absorbers. There had been three different grid sizes used to create coarse, medium, and fine meshes, each with an alternative number of elements. Calculations with varying mesh sizes result in variations in flow output temperature, as shown in Fig. 4. When the mesh size is increased from 0.75 million to 1.25 million, the temperature value rises. There is a very small change in this number from 0.75 to 1.5 million cells. This means there is little influence of mesh density beyond 1.25 million cells. It's demonstrated in Fig.3 , that there are 1.25 million cells in the computational mesh, coupled with finer cells towards the interior layer (c).

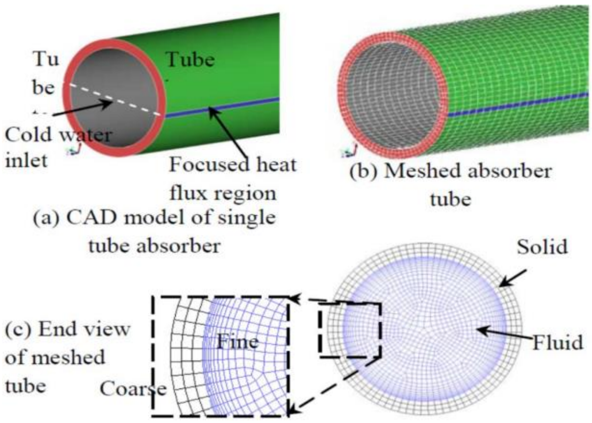

Fig. 3. meshing domain for absorber tube

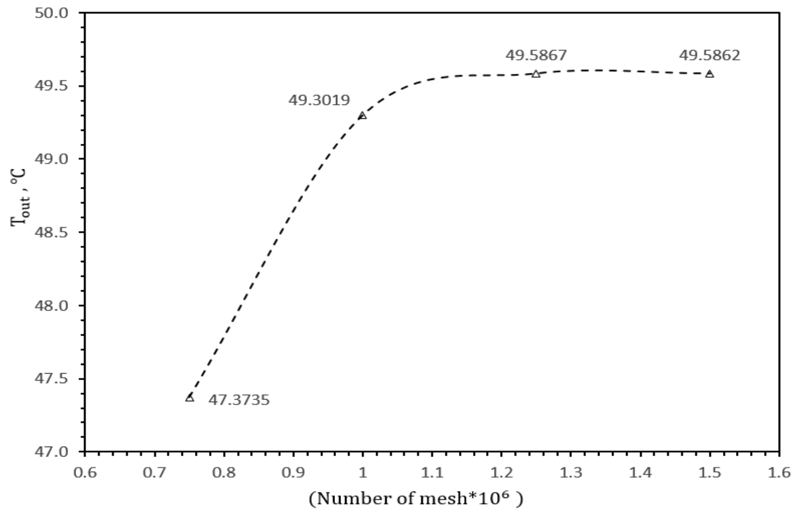

Fig. 4 mesh independence

Convergence

For each model, normalized residuals are used to establish the stability condition. To ensure convergence, all governing partial differential equations and turbulent parameters have scaling standard errors of 10^{-8}. Because all the adjusted error terms have been less than or identical to this desired value, the resolution was said to have been convergent. Once the stability has been attained, the analyses will be completed. Synchronization also isn't reached in all instances. As a consequence, the outcomes don't really change however after 12000 rounds, a condition known as recurrent converging.

Results and discussion

There have been no exceptions to this rule. The temperature of the water had manually determined for each situation. As shown above in Table 1, the solar irradiation and weather conditions both were identical. To begin, the major efficiency and more effectively were clearly described.

Thermal performance

Fig. 5 shows a collector's effectiveness graph. The minimum incidence angles were achieved by aligning direct sun irradiance perpendicular to apertures. Therefore in a situation, the optical productivity will be at its highest level. The comparison of these two curves demonstrates that perhaps the measurement simulation produces results that become near sufficient to those obtained by the computer simulation. A PTC's performance is quite extreme, proving that it is capable of producing water with high temperatures. Most precisely, the collector's efficiency is higher than 75% even under working situations, proving its outstanding performance. In Fig. 6, one can see the absorber's heat loss factor. The radiant loss increased with increasing, so this variable was affected by something like this. Fig. 6 shows the linear relationship between this factor and the quantity $(T_{in}\text{-}T_{am})/G_b$. This parameter features minimum concentrations that can be attributed to the protective film and the vacuum between both the absorbers as well as the covering, respectively. As a result, thermal losses were minimal as well as the loss coefficients were modest, between 0.58 and 1.25. Considering varied working circumstances, Fig. 7 illustrates the heat transfer characteristics within the tubes. Water characteristics, notably dynamic viscosity (μ), oscillate water temperature is changed. There is a convergent boundary between laminar and turbulent flow due to Eq. 1

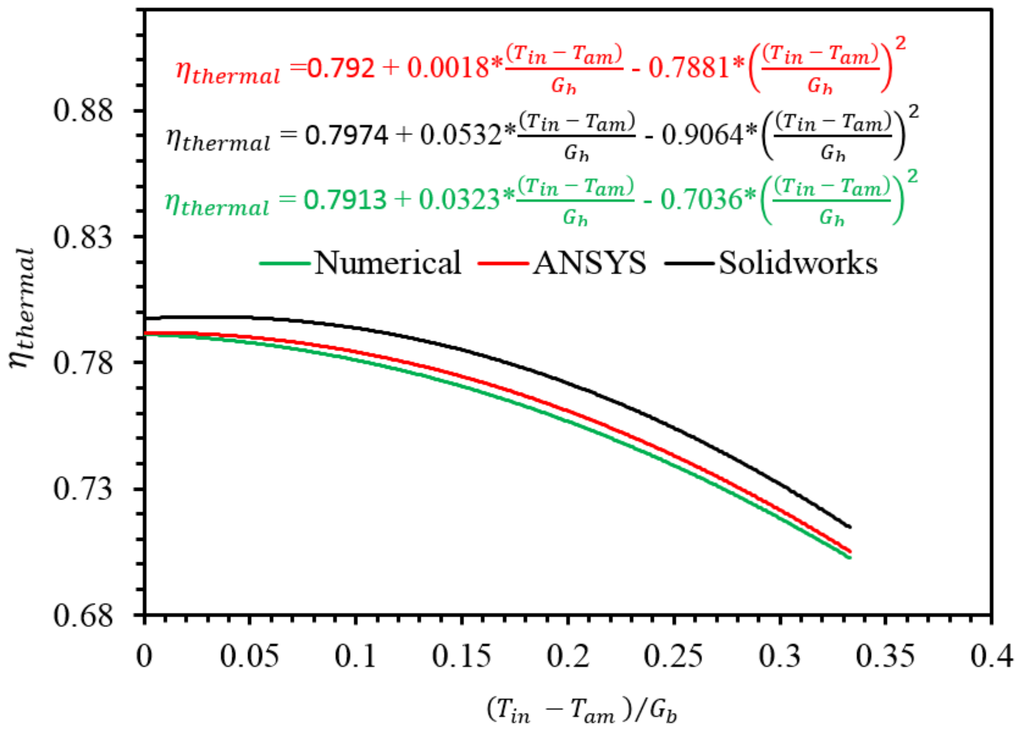

Fig.5 comparison of the collector's thermal efficiency for numerical, solidworks and ANSYS models.

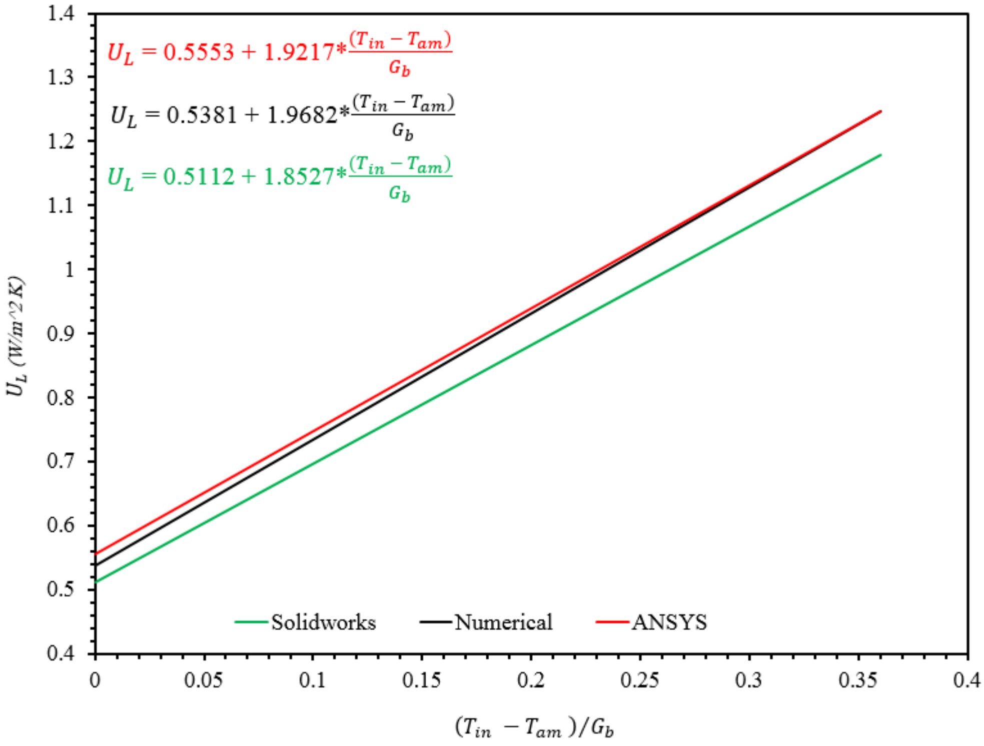

Fig.6 comparison of loss factor for numerical, solidworks and ANSYS models..

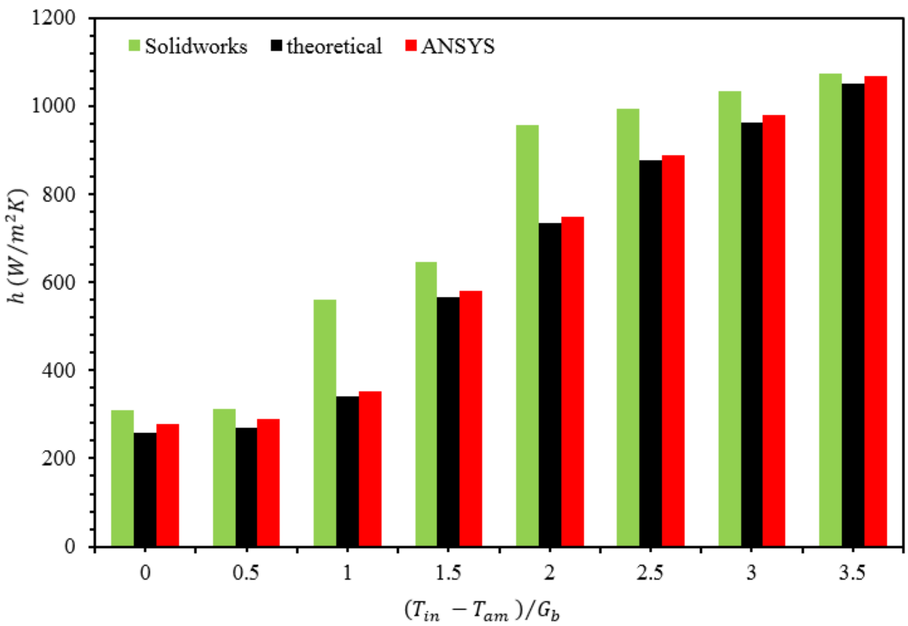

Fig.7 comparison of convective heat transfer coefficient for numerical, solidworks and ANSYS models..

The type of flowing within the pipe has been determined by the Reynolds number within the right axis. Thus long even as water intake temperature is constant, the Reynolds number will vary. Heat transfer coefficients in turbulence,1000 W/m^2 K, are much higher than those in laminar flows (300 W/m^2 K). It demonstrates that turbulence has higher heat transmission properties. As shown in Fig. 7, the thermal factor assumes such an approximate state within a transitional zone. For example, the blue line represents calculations based on Ansys workbench observations, while the red line represents conceptual convective coefficients based on Eq. 8 for the information from different sources of water inflow. As a consequence of the findings being so near to one another, Ansys' results were verified. One thing which confirms these Parametric data is that they have been extremely similar. That demonstrates that turbulence has greater thermal exchange rates.

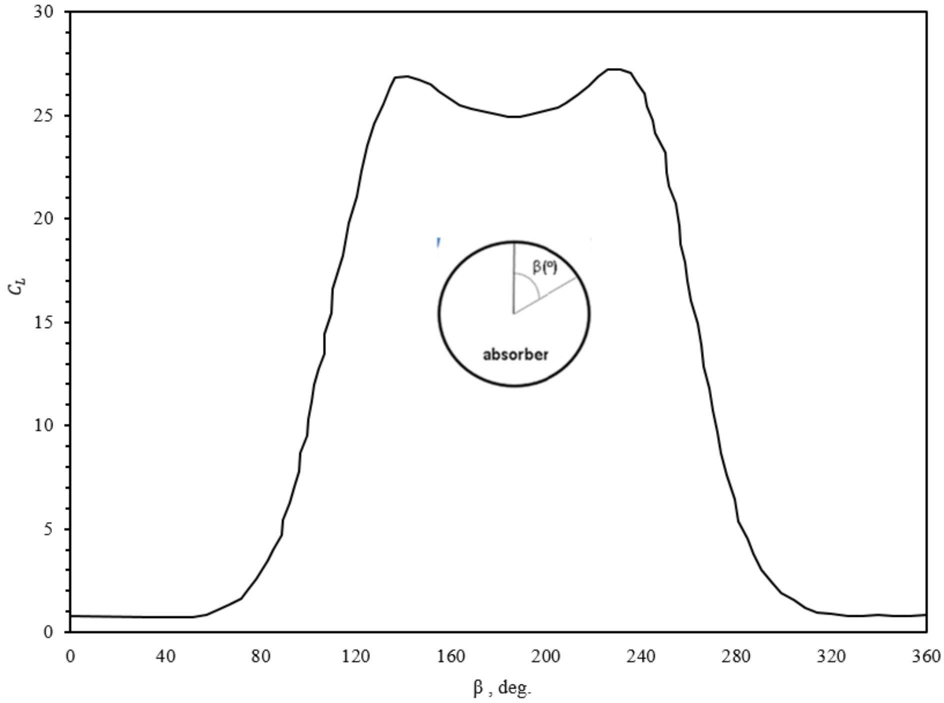

Fig.8 Localized solar energy concentrated on the circmeference of the absorber tube.

As a result of the sunbeams being orthogonal to the apertures that shown in Fig. 8, this concentration of this characteristic also was asymmetrical. Attributed to the reason that no rebounded light reaches small angles, the intensity rate was lower than 1. Particularly, at 135° the quantity is around 27.7 but drops to 25 at 180°. As a result of such rays being focused at the floor of such absorbers, the highest value may be found in the sidewalls of the lowest part. That's close to what it would be if the highest and least localized saturation ratios were averaged out.

According to Fig. 9, the optical efficiency depends on the azimuthal moderator. Whenever the sun rises and sets, the direction of the sunlight varies, which influences the mirrors of such beams. As a result, standard parameters were altered to reverse the trajectory of ray emission to replicate this. As shown in Fig. 9, this variable would be used to simulate this collector on either a daily basis. The optical efficiency decreases as the incidence angle increases, and at angles larger than 68.5°, no beams reach the receivers after the reflection had occurred. Regarding incidence inclinations up to 21.5°, the optical effectiveness modification is more than 0.8, resulting in a satisfactory level of accuracy for such application. Consequently, the collectors require a tracking system to maintain the incidence angle at a minimum.

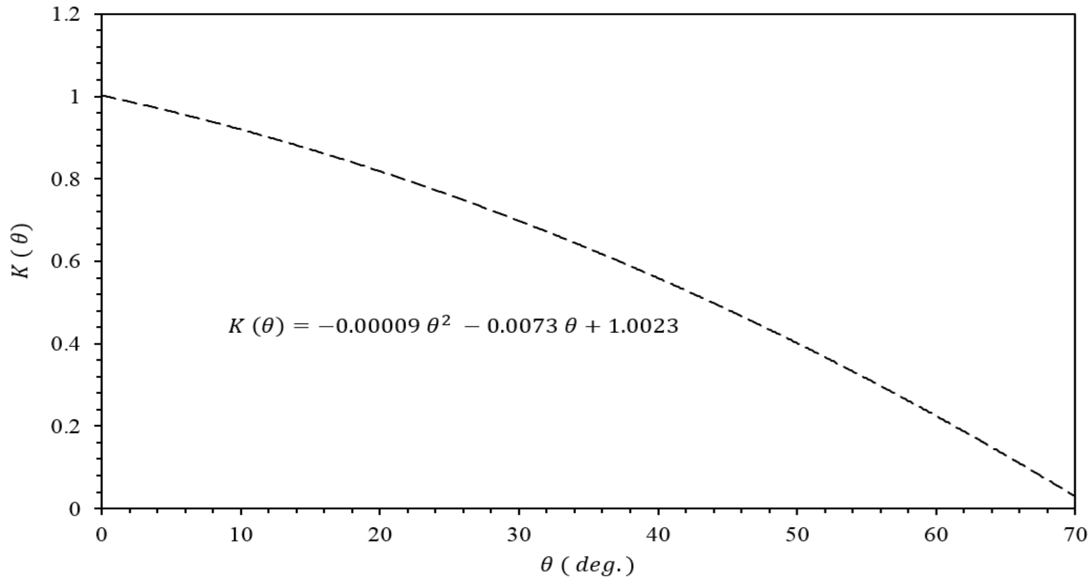

Fig. 9 variation of the optical performance with angular angles.

Heat transfer distribution

Temperature and heat flow dispersion across geometric are seen in this part. It's worth noting that those values below have 93 °C water just at the entrance. Images were obtained from Autodesk's surroundings, and the outcomes were generated using an Ansys workbench. As illustrated in Fig. 10, water is distributed as described in the following:

Water in the pipe bottom becomes hotter since sunlight were focused in one area. A heated tube heats the surrounding water, which then conventionally transfers heat to a tube's middle. Fig. 10 is divided into two halves. The upper portion indicated that the water temperature distributions at five distinct points within the pipe, while the lower section shows the temperature field along with the tube's absorber. According to Fig. 10, red indicates hotter sections of a design. the bottom portion of the tube being the warmest. It's clear from section "b" that now the bottom half of the absorbers was hotter. An increase in temperature is affected by the increased intensity of solar radiation within that location. At 70 percent of its length,

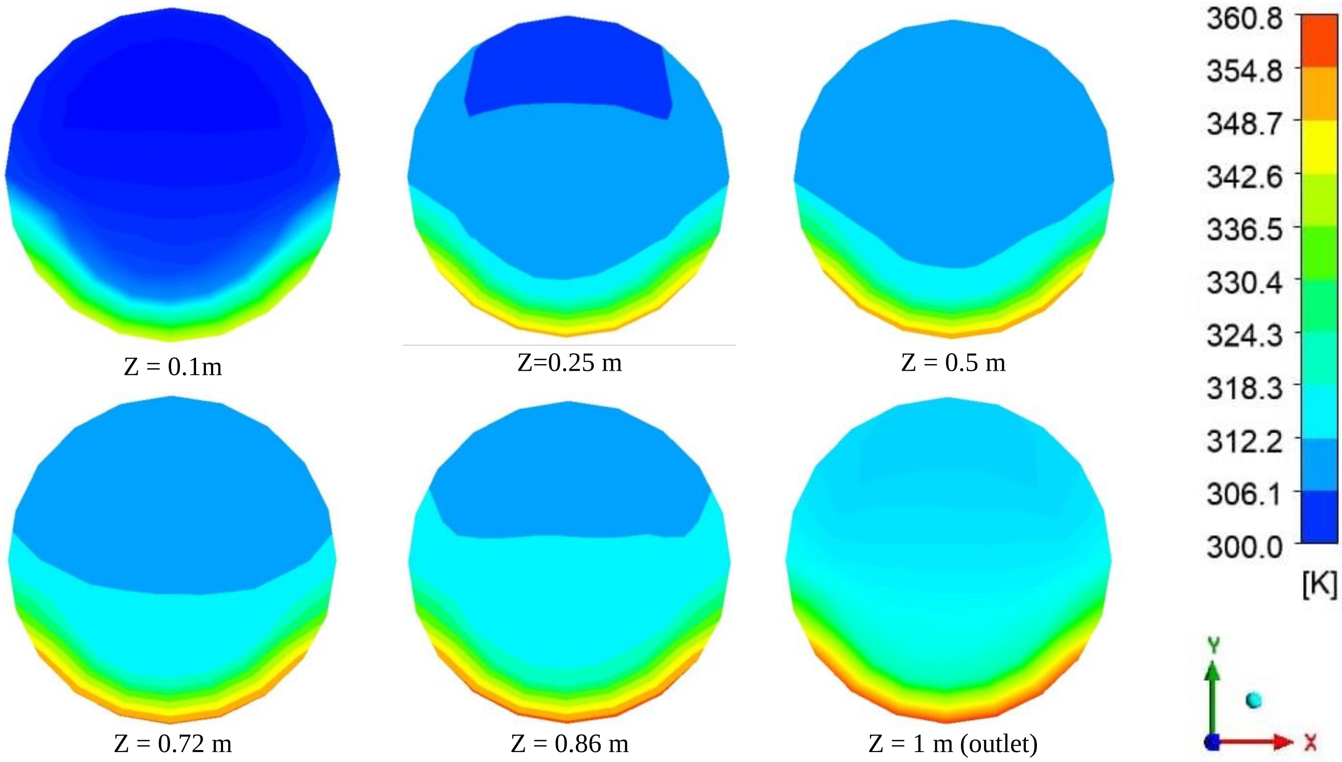

Fig. 10 variation of water bulk temperature in the XY-plane along absorber pipe.

Fig. 11 illustrates the temperature field inside the absorber's face in a cross-section. a tube with a focused radioactive source has the highest value near its lower edge. the temperature difference between upper and lower bounds is just approximately 3 K. This variation is symmetric. The heat flux gradient over the solar collector is shown in the accompanying figure. Readings in blue are higher while those in red were lesser. In the legendary values, there is no physical significance to the opposite sign. On the tube's lowest section, and specifically on its sides, the sun's rays are focused. It is determined by the model's size how exactly the heat source is distributed. Flow simulation modeling enables able to replicate straightforwardly focusing solar arrays and offers a wide range of capabilities to the customers. The improved thermal gradient, incidence angle adjuster of conversion characteristics, and thermal loss coefficient are all included in this paragraph. Ansys can calculate the distribution for temperature of external surface for tube and the amount of water in apartment. With the characteristics of the simulation model, also it is possible to determine the thermal gradient pattern so over receivers at any given point. All of the parameters during every point of something like the model may be known in this approach.

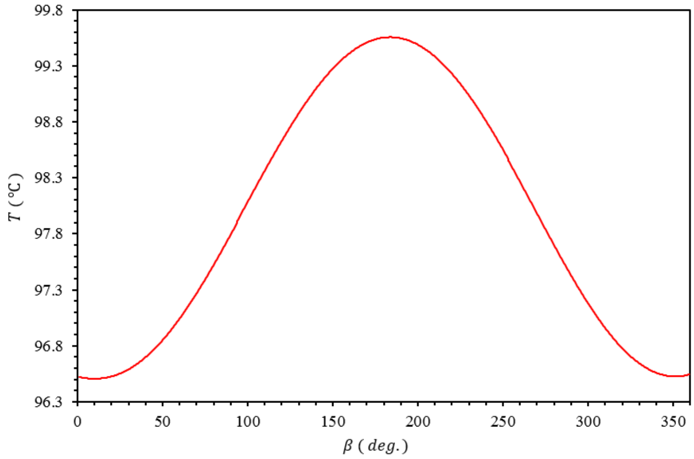

Fig. 11. Profile of surface temperature for the absorber tube.

Conclusions

Ansys is often used to simulate parabolic trough collectors in this analysis. Lab-developed simple numerical simulation validates the outcomes. The simulation's final findings are quite close to the numerical method. When it comes to calculations, there is an emphasis placed on working fluid convective rate, which is why a comparison with the theoretical result is included. Furthermore, Ansys has proven to be a useful tool for users, since it enables users to see these computed numbers at any given point in the models. Moreover, the mathematical model given is novel and yields reliable findings at a cheap cost of processing, which is a major advantage. To get the algorithm to convergence, the relaxed parameter is essential.

The collector's efficiency is about 77.8% at extreme temps, which makes this technique useful. The thermal dissipation rate typically ranges between 0.58 and 1.25 W/mK associated with the input temperature, which is responsible for this high efficiency. The passive solar effects on the development of an absorber tube would be the next essential characteristic to study since it influences the temperature profile of the absorbent's surfaces. Around 45 degrees from the vertical plane, the highest concentration ratio of renewable radiation may well be noticed upon that lower portion of the absorbers. There is also a large difference between the highest localized concentration range of 27.7 and the average of 13.15, whereas the top half quantity was approximately around 1.

Because of the thermal gradient composition and distribution, the warmest section of the absorbers is usually located at the base. There's roughly a 5 K difference temperature inside a radius all around absorbers. Transverse temperature distributions of water demonstrate that water is hotter in lower sections due to a higher absorption coefficient.

To maximize the effectiveness of a solar concentrator, the directions of such ultraviolet irradiance is crucial, primarily for optically component. Larger incidence angles cause higher-end inefficiencies within collectors, reducing efficiency. As long as the incidence angle is less than 21.5 degrees, the angle efficiency modifier is more than 0.84, and the collector’s efficiency is excellent. As soon as the absorbers hit 68.5°, the amount of solar radiation that reaches it is insufficient to produce usable energy, as well as the collection cannot function.

The computation of the thermal performance formula, as well as the optically modification ratio, allows users to understand the collector's performance under various resources and strategies, which is crucial to note. It is therefore possible to import that model into yet another predictive algorithm or programming using the formulas from this design.

References

[1] K. Nithyanandam, R. Pitchumani, Optimization of an encapsulated phase change material thermal energy storage system, Sol. Energy 107 (2014), 770–788.

[2] N.S. Suresh, N.C. Thirumalai, Badri S. Rao, M.A. Ramaswamy, Methodology for sizing the solar field for parabolic trough technology with thermal storage and hybridization, Sol. Energy 110 (2014) 247–259.

[3] Gur Mittelman, Michael Epstein, A novel power block for CSP systems, Sol. Energy 84 (10) (2010) 1761–1771.

[4] A. FernلJndez-Garcي a, E. Zarza, L. Valenzuela, M. Pérez, Parabolic-trough solar collectors and their applications, Renew. Sustain. Energy Rev. 14 (2010), 1695–1721.

[5] K. Zabara, Estimation of the global solar radiation in Greece, Sol. Wind Technol. 3 (4) (1986) 267–272.

[6] D.A. Kouremenos, K.A. Antonopoulos, E.S. Domazakis, Solar radiation correlations for the Athens, Greece, area, Sol. Energy. 35 (3) (1985) 259–269.

[7] D. Kruger, Y. Pandian, et al., Parabolic trough collector testing in the frame of the REACt project, Desalination 220 (1–3) (2008) 612–618.

[8] R. Grena, Optical simulation of a parabolic solar trough collector, Int. J. Sustain. Energy 29 (1) (2010) 19–36.

[9]] H. Price, E. Lópfert, D. Kearney, E. Zarza, G. Cohen, R. Gee, et al., Advances in parabolic trough solar power technology, J. Sol. Energy Eng. 124 (2002), 109–125.

[10] Marco Binotti, Guangdong Zhu, Allison Gray, Giampaolo Manzolini, Paolo Silva, Geometric analysis of three-dimensional effects of parabolic trough collectors, Sol. Energy 88 (2013) 88–96.

[11] J.A. Clark, An analysis of the technical and economic performance of a parabolic trough concentrator for solar industrial process heat application, Int. J. Heat Mass Transf. 25 (9) (1982) 1427–1438.

[12] S. Al-Soud Mohammed, S. Hrayshat Eyad, A 50 MW concentrating solar power plant for Jordan, J. Clean. prod. 17 (2009) 625–635.

[13] N. El Gharbi, H. Derbal, S. Bouaichaoui, N. Said, A comparative study between parabolic trough collector and linear Fresnel reflector technologies, Energy Proc. 6 (2011) 565–572.

[14] T. Boukelia, M.S. Mecibah, Parabolic trough solar thermal power plant: potential, and projects development in Algeria, Renew. Sustain. Energy Rev. 21 (2013) 288–297.

[15] W. Grasse, Solar PACES Annual Report, DLR, Germany, 1995.

[16] Malika Ouagued, Abdallah Khellaf, Larbi Loukarfi, Estimation of the temperature, heat gain and heat loss by solar parabolic trough collector under Algerian climate using different thermal oils, Energy Convers. Manag. 75 (2013) 191–201.

[17] Ze-Dong Cheng, Ya-Ling He, Bao-Cun Du, Kun Wang, Qi Liang, Geometric optimization on optical performance of parabolic trough solar collector systems using particle swarm optimization algorithm, Appl. Energy 148 (2015) 282–293.

[18] A. de Risi, M. Milanese, D. Laforgia, Modelling and optimization of transparent parabolic trough collector based on gas-phase nanofluids, Renew. Energy 58 (2013) 134–139. October.

[19] A. Hachicha, I. Rodrيguez, O. Lehmkuhl, A. Oliva, On the CFD&HT of the flow around a parabolic trough solar collector under real working conditions, Energy Proc. 49 (2014) 1379–1390.

[20] Z.D. Cheng, Y.L. He, F.Q. Cui, B.C. Du, Z.J. Zheng, Y. Xu, Comparative and sensitive analysis for parabolic trough solar collectors with a detailed Monte Carlo ray tracing optical model, Appl. Energy 115 (15) (2014) 559–572.

[21] T. Sokhansefat, A.B. Kasaeian, F. Kowsary, Heat transfer enhancement in parabolic trough collector tube using Al2O3/synthetic oil nanofluid, Renew. Sustain. Energy Rev. 33 (2014) 636–644.

[22] Hongbo Liang, Shijun You, Huan Zhang, Comparison of different heat transfer models for parabolic trough solar collectors, Appl. Energy 148 (2015)105–114.

[23] Fritz Zaversky, Rodrigo Medina, Javier Garcيa-Barberena, Marcelino SلJnchez, David Astrain, Object-oriented modeling for the transient performance simulation of parabolic trough collectors using molten salt as heat transfer fluid, Sol. Energy 95 (2013) 192–215.

[24] Ze-Dong Cheng, Ya-Ling He, Yu Qiu, A detailed nonuniform thermal model of a parabolic trough solar receiver with two halves and two inactive ends, Renew. Energy 74 (2015) 139–147.

[25] G.J. Gong, X.Y. Huang, J. Wang, M.L. Hao, An optimized model and test of the China's first high temperature parabolic trough solar receiver, Sol. Energy 84 (2010) 2230–2245.

[26] Acine Marif, Hocine Benmoussa, Hamza Bouguettaia, Mohamed M. Belhadj, Moussa Zerrouki, Numerical simulation of solar parabolic trough collector performance in the Algeria Saharan region, Energy Convers. Manag. 85 (2014) 521–529.

[27] Yanjuan Wang, Qibin Liu, Jing Lei, Hongguang Jin, Performance analysis of a parabolic trough solar collector with non-uniform solar flux conditions, Int. J. Heat Mass Transf. 82 (2015) 236–249.

[28] Ze-Dong Cheng, Ya-Ling He, Kun Wang, Bao-Cun Du, F.Q. Cui, A detailed parameter study on the comprehensive characteristics and performance of a parabolic trough solar collector system, Appl. Therm. Eng. 63 (2014) 278–289.

[29] Yanjuan Wang, Qibin Liu, Jing Lei, Hongguang Jin, A three-dimensional simulation of a parabolic trough solar collector system using molten salt as heat transfer fluid, Appl. Therm. Eng. 70 (2014) 462–476.

[30] M. Eck, J.F. Feldhoff, R. Uhlig, Thermal modelling and simulation of parabolic trough receiver tubes, in: Proceedings of the ASME 2010 4th International Conference on Energy Sustainability, Phoenix, 2010.

[31] Li Xu, Zhifeng Wang, Xin Li, Guofeng Yuan, Feihu Sun, Dongqiang Lei, Dynamic test model for the transient thermal performance of parabolic trough solar collectors, Sol. Energy 95 (2013) 65–78.

[32] Esmail M.A. Mokheimer, Yousef N. Dabwan, Mohamed A. Habib, Syed A.M. Said, Fahad A. Al-Sulaiman, Techno-economic performance analysis of parabolic trough collector in Dhahran, Energy Convers. Manag. 86 (2014) 622–633.
[33] İbrahim Halil Yılmaz, Mehmet Sait S◌̦ylemez, Thermo-mathematical modeling of parabolic trough collector, Energy Convers. Manag. 88 (2014) 768–784.
[34] Soteris A. Kalogirou, A detailed thermal model of a parabolic trough collector receiver, Energy 48 (1) (2012) 298–306.
[35] Chung-Yu Tsai, Psang Dain Lin, Optimized variable-focus-parabolic-trough reflector for solar thermal concentrator system, Sol. Energy 86 (5) (2012), 116 4 –1172.
[36] S.M. Akbarimoosavi, M. Yaghoubi, 3D Thermal-structural Analysis of an Absorber Tube of a Parabolic Trough Collector and the Effect of Tube Deflection on Optical Efficiency, Energy Proc. 49 (2014) 2433–2443.
[37] P. Mohammad Zadeh, T. Sokhansefat, A.B. Kasaeian, F. Kowsary, A. Akbarzadeh, Hybrid optimization algorithm for thermal analysis in a solar parabolic trough collector based on nanofluid, Energy 82 (2015) 857–864.
[38] Ya-Ling He, Jie Xiao, Ze-Dong Cheng, Yu-Bing Tao, A MCRT and FVM coupled simulation method for energy conversion process in parabolic trough solar collector, Renew. Energy 36 (2011) 976–985.
[39] Z.D. Cheng, Y.L. He, J. Xiao, Y.B. Tao, R.J. Xu, Three-dimensional numerical study of heat transfer characteristics in the receiver tube of parabolic trough solar collector, Int. Commun. Heat Mass Transf. 37 (2010) 782–787.
[40] Aggrey Mwesigye, Tunde Bello-Ochende, Josua P. Meyer, Heat transfer and thermodynamic performance of a parabolic trough receiver with centrally placed perforated plate inserts, Appl. Energy 136 (2014) 989–1003.
[41] Victor C. Pigozzo Filho, Alexandre B. de Sل, J. lio C. Passos, Sergio Colle, Experimental and Numerical Analysis of Thermal Losses of a Parabolic Trough Solar Collector, Energy Proc. 57 (2014) 381–390.
[42] Liang Zhang, Zitao Yu, Liwu Fan, Wujun Wang, Huan Chen, Yacai Hu, Jianren Fan, Mingjiang Ni, Kefa Cen, An experimental investigation of the heat losses of a U-type solar heat pipe receiver of a parabolic trough collector-based natural circulation steam generation system, Renew. Energy 57 (2013) 262–268.
[43] Liang Zhang, Wujun Wang, Zitao Yu, Liwu Fan, Yacai Hu, Yu Ni, Jianren Fan, Kefa Cen, An experimental investigation of a natural circulation heat pipe system applied to a parabolic trough solar collector steam generation system, Sol. Energy 86 (2012) 911–919.
[44] X. Xiao, P. Zhang, D.D. Shao, M. Li, Experimental and numerical heat transfer analysis of a V-cavity absorber for linear parabolic trough solar collector, Energy Convers. Manag. 86 (2014) 49–59.
[45] Loreto Valenzuela, Rafael L◌́pez-Martين, Eduardo Zarza, Optical and thermal performance of large-size parabolic-trough solar collectors from outdoor experiments: a test method and a case study, Energy 70 (2014) 456–464.
[46] V.E. Dudley, G.J. Kolb, M. Sloan, D. Kearney, Test Results: SEGS LS-2 Solar Collector, Report of Sandia National Laboratories (SAND94-1884), 1994.
[47] J. Leinhard IV, J. Leinhard V, A Heat Transfer Textbook, 4th edition . Philogiston Press, USA, 2012, 354–360.
[48] M. S. Mahmoud, “Numerical investigation of conjugate combined convective heat transfer for internal laminar flow of Al2O3/water nanofluid through tube - Flat plate solar collector,” J. Eng. Sci. Technol., vol. 16, no. 3, pp. 2378–2393, 2021.
[50] Khudheyer, Ahmed F. 2020. "Numerical investigation and exergetic analysis of convergent-divergent absorber tube in concentrated solar trough. Journal of Green Engineering, 10(10), 8083-8104.
[51] Mahmoud, S., Abbas, A.; and Khudheyer, Ahmed F. 2020. "Solar parabolic trough collector tube heat transfer analysis with internal conical pin fins". Journal of Green Engineering, 10(10), 7422-7436.
[52] Abbas, A., Mahmoud, S.M., and Khudheyer, Ahmed F., 2020. "Improvement of heat transfer for airflow through a solar air heater channel with cut-off desecrate baffles". Journal of Green Engineering, 10(7), 4292-4308.
[53] Mahmoud Sh. Mahmoud, Khudheyer, Ahmed F. 2020. "A Novel design of the solar central receiver to improve the performance of the central solar power tower plant". IOP Conf. Ser.: Mater. Sci. Eng. 928 022003. doi:10.1088/1757-899X/928/2/022003